FULL PAPERS

Mesoporous Titania Thin Film with Highly Ordered and Fully Accessible Vertical Pores and Crystalline Walls

Chol-Won Koh,[b] U-Hwang Lee,[c] June-Kyu Song,[b] Hae-Rim Lee,[b] Min-Hye Kim,[b] Myungkoo Suh,[d] and Young-Uk Kwon*[a, b, c, d]

Abstract: We report the preparation of mesoporous titania thin films with the $R\bar{3}m$ pore structure derived from the $Im\bar{3}m$ self-assembled ordering of the titania species and an $EO_{106}PO_{70}EO_{106}$ triblock copolymer. The films were spin-cast and then aged at 18 °C at a relative humidity of 70 %, which led to the orientation of the $Im\bar{3}m$ structure with the [111] direction perpendicular to the substrates. The [111] body-diagonal channels became vertical channels upon calcination at 400 °C, thus leading to thin films with vertical channels. The pores are ordered over a large area of up to 1 µm². The titania films can be formed on various types of substrates.

Keywords: mesoporous materials · thin films · titania · rhombohedral structures · vertical channels

By using a titania film formed on a Pt-coated Si wafer as a template, we produced by an electrochemical-deposition technique arrays of gold nanowires, whose morphology suggests that most of the pores of the titania thin films are accessible. The pore structure of vertical channels is stable up to 600 °C, at which temperature the wall materials crystallize into anatase.

Introduction

Mesoporous titania thin films (MTTFs)[1–4] with ordered pores are unique because they have many interesting and useful features, such as homogeneous nanometer-sized pores, large surface areas, the many useful physicochemical properties of titania, and the thin-film form, all combined into one body. These make MTTFs ideal candidates for the development of novel nanomaterials and nanodevices.[5,6]

[a] Prof. Dr. Y.-U. Kwon
SKKU Advanced Institute of Nanotechnology
Sungkyunkwan University
Suwon, 440-746 (Korea)
Fax: (+82)31-290-7070
E-mail: ywkwon@skku.edu

[b] C.-W. Koh, J.-K. Song, H.-R. Lee, M.-H. Kim, Prof. Dr. Y.-U. Kwon
Department of Chemistry, BK-21
School of Chemical Materials Science
Sungkyunkwan University
Suwon, 440-746 (Korea)

[c] Dr. U.-H. Lee, Prof. Dr. Y.-U. Kwon
Center for Nanotubes and Nanostructured Composites
Sungkyunkwan University
Suwon, 440-746 (Korea)

[d] Dr. M. Suh, Prof. Dr. Y.-U. Kwon
Institute of Basic Science
Sungkyunkwan University
Suwon, 440-746 (Korea)

Functional hybrid materials with regular nanostructures can be realized by incorporating various organic or inorganic materials into the pores of MTTFs.[7–9]

To use MTTFs for such purposes, several requirements need to be satisfied. First, the pores must be accessible from the outside.[10] Unlike powder, the internal space of a mesoporous thin film may not be accessible unless there are pore openings at the surfaces. Several different approaches have been attempted to produce mesoporous thin films with accessible pores, including pore alignment with an applied magnetic field[10] or modification of the substrate surfaces.[11] Wu et al. reported that MTTFs with a 3D hexagonal ($P6_3/mmc$) structure could be processed into a structure with vertical pores.[12] However, it seems that a more general and practical way is the formation of mesoporous thin films with isotropic pore structures. In this regard, the synthesis of cubic-structured MTTFs with oriented pores is an important first step for the development of MTTF-based nanodevices.[13] Second, crack-free thin films with large ordered domains are important to ensure reproducible device performance. Third, a high degree of wall crystallinity would be desirable to make use of most of the physical properties of titania. Fourth, it would be beneficial if an MTTF can be formed on various substrates without changing the pore structure for a wide range of applications. Although some MTTFs reported in the literature show one or two of these

properties, there has been no account of MTTFs that show all these features simultaneously.

Herein, we report a new MTTF in which the pore structure can be described as an ordered array of vertical channels whose domains are larger than $1 \times 1 \, \mu m^2$. The vertical channels with open ends ensure that all the pores are accessible from the surface, thus allowing further fabrication into nanostructured materials or nanodevices. Furthermore, our MTTFs can be formed on various types of substrates, including metallic substrates. This enabled us to form nanostructured materials inside the pores by electrochemical deposition. We demonstrate this possibility by growing nanostructured gold inside the pores of our MTTF. Because most of the pores are accessible, we could synthesize high-density arrays of nanomaterials, which may be the first step towards the fabrication of nanostructured materials based on MTTFs.

Results and Discussion

MTTFs with ordered channels were formed by spin-coating a precursor solution of $TiCl_4$ and a Pluronic nonionic block copolymer F-127 ($EO_{106}PO_{70}EO_{106}$, EO = ethylene oxide, PO = propylene oxide) in ethanol onto substrates at 25 °C, followed by aging at 18 °C for 72 h and calcination at 400 °C. For reproducible synthesis, we tried various combinations of temperature and humidity levels and established the optimum conditions for each step as described in the Experimental Section. We used various types of substrates, including glass slides, indium tin oxide, fluorine-doped tin oxide, and Pt- or Au-coated Si wafers, and confirmed that the pore structure and pore orientation were not influenced by the nature of the substrate.

Figure 1 shows the scanning electron microscopy (SEM) images of our MTTFs from various viewing angles. The film thickness could be controlled from 150 to 500 nm (Figure 1b and c) by using different spinning speeds during the spin-coating step. The thicker film was obtained from 4000 rpm, and the thinner one from 6000 rpm. Regardless of the film thickness, the SEM images all show that the pores are well-ordered over a large area ($> 1 \times 1 \, \mu m^2$), which indicates the preferential orientation of the pores. The top-view (Figure 1a) and tilted-view (Figure 1c) images show that there are open pores at the film surface, which are ordered with hexagonal symmetry. Both the side-view (Figure 1b) and tilted-view (Figure 1c) images show that there are vertically
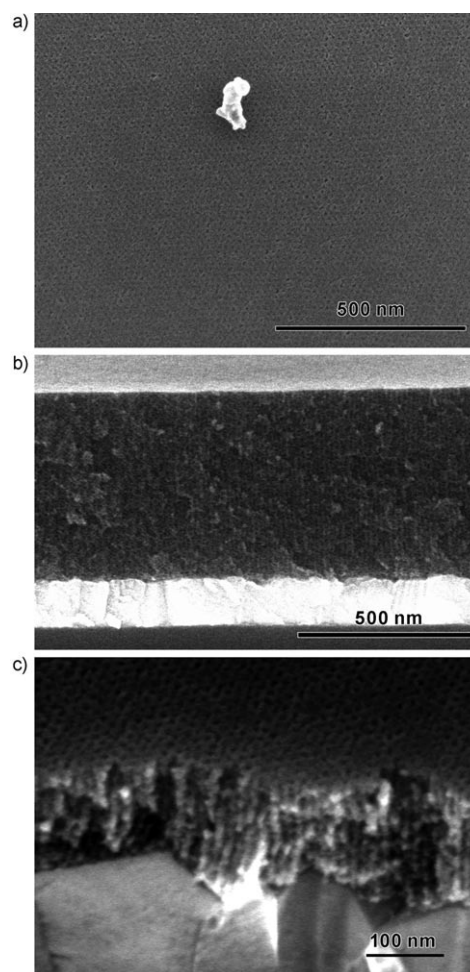

Figure 1. Field-emission SEM (FESEM) images of a mesoporous titania thin film. a) Top view; b) side view; c) tilted view.

aligned parallel channels. These images collectively show that our MTTFs have vertical channels with hexagonal symmetry.

There are only two possible ways to explain the pore structure in Figure 1. One is a *p6mm* hexagonal mesoporous structure with the channels standing vertically, and the other is a cubic structure (or its rhombohedral derivative) with the [111] direction oriented vertically. We can rule out the first possibility on the basis of the following reasons: First, a perpendicular orientation of the channels of the *p6mm* structure relative to the substrate is highly unlikely because such an orientation will create a large amount of surface energy at the interface. To overcome this problem, Yamauchi et al. applied a very strong magnetic field to align the channels, but the alignment was not perfect.[10] Koganti et al. showed that modification of the substrate surface with a Pluronic block copolymer could lower the surface energy and induce the channels to tilt away from the substrate plane, but the resultant channels were not perpendicular.[11] In the present study, we did not use such measures to induce vertical alignment of the pores. Second, the channel walls are not straight

Abstract in Korean:

이산화티탄 입자와 $EO_{106}PO_{70}EO_{106}$ 블록고분자의 *Im-3m* 자기조립으로부터 유도된 *R-3m* 구조를 갖는 메조동공 이산화티탄 박막으로 합성하였다. 이 박막은 스핀-코팅과 상대 습도 70%, 18℃ 의 조건에서 숙성 과정을 거쳐 합성된다. 숙성 과정 중에 박막은 [111] 방향이 기판에 수직 되게 배향 하게 된다. 400℃ 에서 소성시키면 이 [111] 체심 대각선 방향의 채널이 수직 채널이 된다. 이와 같은 동공은 1 μm^2 범위까지 잘 배열된 구조를 보인다. 이러한 박막은 다양한 기판 위에 형성될 수 있다. 우리는 백금 박막이 입혀진 실리콘 웨이퍼 위에 메조동공 이산화티탄 박막을 형성하고 이를 주형으로 이용하여 전기화학적 방법으로 나노구조 금을 형성하였다. 이 나노구조 금의 형상으로 보아 이산화티탄 박막의 거의 모든 동공은 외부 에서 접근 이 가능한 것으로 보인다. 이 박막의 동공구 조는 600℃ 로 가열하여도 유지되며, 이 때 동 공벽 물질은 anatase 로 결정 화된다.

as would be expected from the *p6mm* pore structure, but are periodically modulated in such a way that each channel can be described as being composed of periodically arranged cages and connecting necks between the neighboring cages. Therefore, we conclude that the pore structure of our MTTFs are derived from a cubic structure with its [111] direction oriented vertically.

As sol–gel thin films are bound to experience vertical shrinkage during the aging and calcination steps, and the direction of shrinkage coincides with the [111] direction of the cubic structure in the present MTTFs, the pore structure is thus likely to be rhombohedral.

Transmission electron microscopy (TEM) images taken along various directions of our MTTF are shown in Figure 2. These images can be well-explained with a rhombohedral unit cell with $a \approx 12.5$ nm and $\alpha \approx 100°$. The average pore-to-pore distance measured from the [111]-view TEM image (Figure 2c) was 11 nm, which corroborates with the top-view SEM image (Figure 1a). These images and the TEM images of electrochemically grown nanostructured gold inside the pores show that the pores are connected and cagelike (Figure 5). With these observations, the parent structure of the present rhombohedral structure was determined to be $Im\bar{3}m$.[14,15] The contraction along the [111] direction from the $Im\bar{3}m$ structure causes the loss of the four-fold symmetry while preserving the threefold symmetry along the [111] direction. Therefore, we singled out the space group $R\bar{3}m$, a maximal nonisomorphic subgroup of $Im\bar{3}m$, for our MTTFs. Choi et al. reported the formation of an $R\bar{3}m$-structured MTTF.[14] However, the pores in their films are isolated, in contrast to ours.

The low-angle XRD pattern of the calcined film (Figure 3) shows only three peaks with $d = 9.7$, 4.9, and 2.3 nm. With the estimated lattice parameters and the rhombohedral crystal system deduced from the SEM and TEM data, these peaks could be indexed as $(0\bar{1}1)$, $(0\bar{2}2)$, and $(0\bar{4}4)$, respectively. The appearance of only a series of $(0\bar{k}k)$ peaks is consistent with the preferred orientation discussed above. The absence of any (hhh) reflection can be explained with the structure derived from the $Im\bar{3}m$ structure. Unfortunately, the limited number of XRD peaks prohibits any further precise determination of the lattice parameters from those estimated from the SEM and TEM data.

Figure 4 shows schematic drawings of how the vertical channel structure of our MTTFs are formed. The surfactant and titania precursor in the as-cast film self-assemble into an $Im\bar{3}m$ structure. The surfactant micelles form cage pores. The key factor of our synthesis is that the pores are ordered with the [111] direction perpendicular to the film surface. Calcination of this film not only removes surfactant but also shrinks the film in the vertical direction. Because of the [111] orientation, the direction of shrinkage coincides with the [111] direction of the cubic unit cell. The contraction induces a structural transformation into the rhombohedral ($R\bar{3}m$) structure. The contraction also connects the pores to their neighbors along the [111] direction, thus producing vertical channels. The various dimensions measured by the
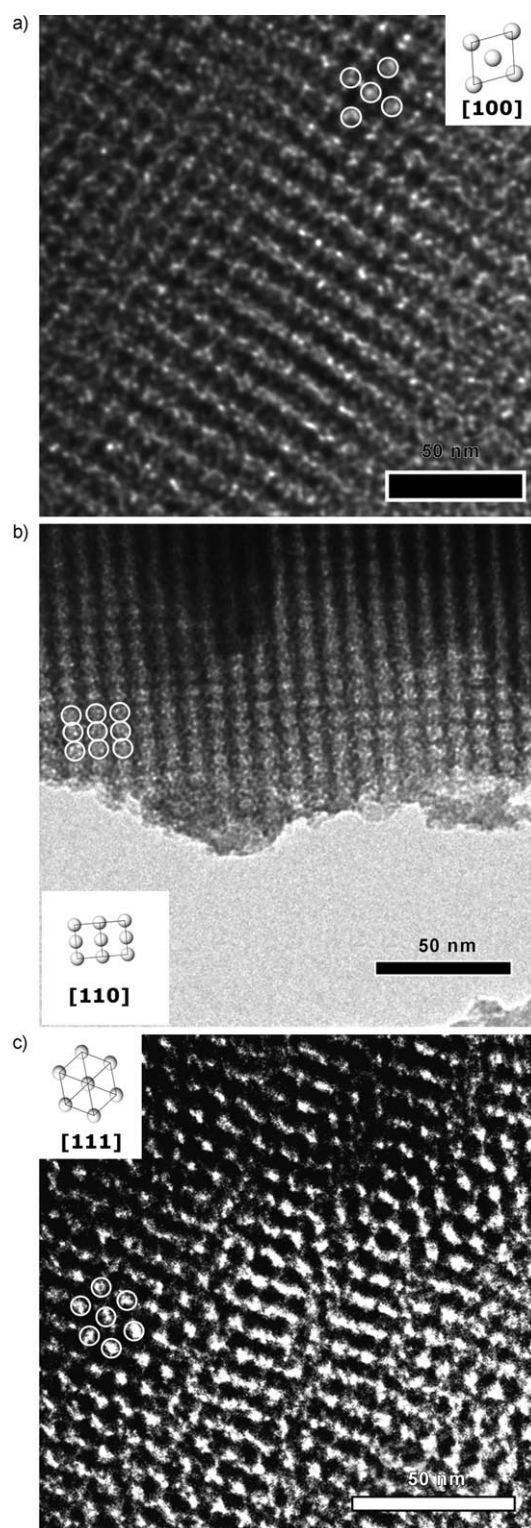

Figure 2. TEM images of a mesoporous titania thin film. a) [100] view; b) [110] view; c) [111] view. Some pores are marked with white circles for easy comparison with the simulated models in the insets. The models are slightly tilted to match the images.

characterization methods mentioned above are all consistent with this scheme.
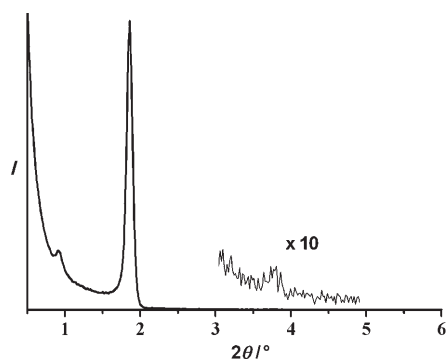
Figure 3. Low-angle XRD pattern of a mesoporous titania thin film obtained by calcination at 400°C.
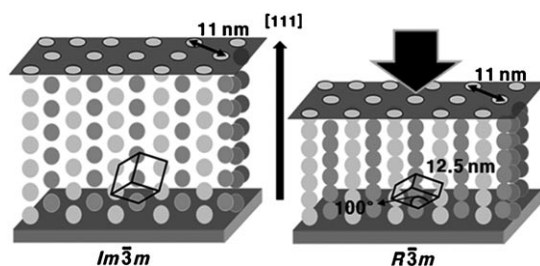

Figure 4. Schematic representation of the structure of a mesoporous titania thin film before (left) and after calcination (right).

Through a similar approach, Crepaldi et al.[2] also reported an MTTF whose structure was derived from the $Im\bar{3}m$ ordering. However, in their case, the direction of preferred orientation was [110]. The thermal contraction along the [110] direction resulted in a $C2m$ structure, which did not have vertical channels. The pore accessibility was not mentioned in the paper. It is interesting that their synthesis and ours both produced the same $Im\bar{3}m$ structure in the as-cast states but with two different orientations. There may be many factors that make such a subtle difference. We believe that the most fundamental factor is the method of film formation. We used the spin-casting method followed by aging to obtain the ordered mesostructure, whereas Crepaldi et al. used dip-coating. In the latter case, the evaporation-induced self-assembly (EISA) mechanism[17] is in operation, in which mesoscale ordering is achieved almost instantly after the film material is withdrawn from the solution. On the contrary, spin-coating generally does not yield such a high degree of mesoscopic ordering. This is probably because the faster solvent evaporation in the spin-coating method makes the film material more viscous, which in turn makes the movement of the titania and surfactant species too sluggish to achieve a high degree of ordering in a short period of time. Therefore, even if the self-assembled structure may form by spin-coating, the degree of ordering cannot be as high as in the case with dip-coating. The ordering can be improved by aging under controlled conditions of temperature and hu-

midity. In our previous paper, we showed that the mesoscale ordered structures could be tuned by employing different temperatures for the aging step.[3,5] This suggests that the film materials in the aging step are liquid-crystal-like, and that the ordering is achieved by the movement of titania particles and surfactant molecules to attain the most thermodynamically stable ordering and orientation under the given conditions. With the largest exposed surface of the micelles facing the interfaces, the [111] orientation appears to be the most thermodynamically favored orientation for the $Im\bar{3}m$ mesostructured film, which explains the ordering of our films. The [110] orientation from the dip-coating procedure, therefore, appears to be a kinetically stabilized structure. The adaptability of our method to a wide range of substrates appears to originate from the thermodynamic nature of the process.

The vertical channels in large domains of our MTTFs, combined with their ability to form on conducting substrates, provide a unique opportunity to grow arrays of nanomaterials with the electrochemical-deposition technique. Figure 5 shows the TEM images of one such example, in which nanostructured gold was grown inside the channels in high density and with a high degree of homogeneity. For this, we formed an MTTF on a Pt-coated Si wafer and used it as an electrode. As shown in these images, almost all the pores were filled with gold, thus forming arrays of connected nanoparticles embedded inside the MTTF. However, some pores are not filled with gold (Figure 5b). This may be unavoidable, probably due to the stochastic nature of the electrochemical deposition and the inaccessibility of some of the pores. The high-magnification TEM image in Figure 5c shows the lattice fringe patterns of the deposited gold, which indicates high crystallinity. It also shows that the dimension of each gold nanoparticle is about 7 nm, which sets the lowest limit of pore dimension for our MTTFs. The gold spheres are connected with neighboring ones through narrow necks, in agreement with the cagelike pore structure described above. The unprecedented high density of gold nanorod replicas inside the pores of the MTTF is a direct consequence of the vertical open channels with large domains of our MTTFs.

Additionally, we found that the calcination temperature could be raised to 600°C without losing the pore ordering. Figure 6 shows the wide-angle XRD and TEM data of an MTTF calcined at 500°C. Figure 6a shows that the film material is crystalline anatase. The TEM image in Figure 6b shows that the long-range mesoporous structure of our MTTF was maintained. Figure 6c shows that all the wall material had turned into a crystalline phase, which was identified as anatase by the electron-diffraction pattern (Figure 6d). In general, crystallization of the titania wall requires the calcination temperature to be higher than 400°C, a temperature at which most non-silica mesoporous structures collapse. Special measures were employed to circumvent this problem.[18,19] In this regard, it is remarkable that our MTTF does not lose its mesoporous structure while attaining a high degree of crystallinity. On the other hand, the
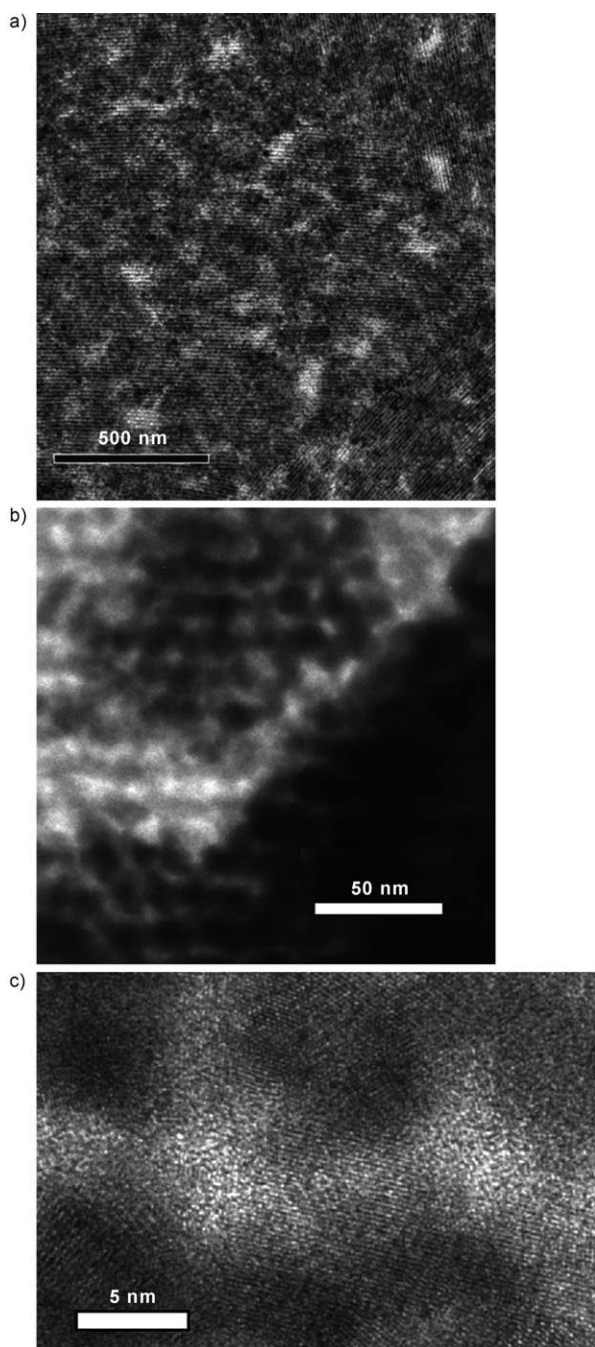
a)

b)

c)

Figure 5. TEM images of various magnifications: a) 40 000, b) 320 000 and c) 2 800 000 of a mesoporous titania thin film with nanostructured gold grown inside the pores.
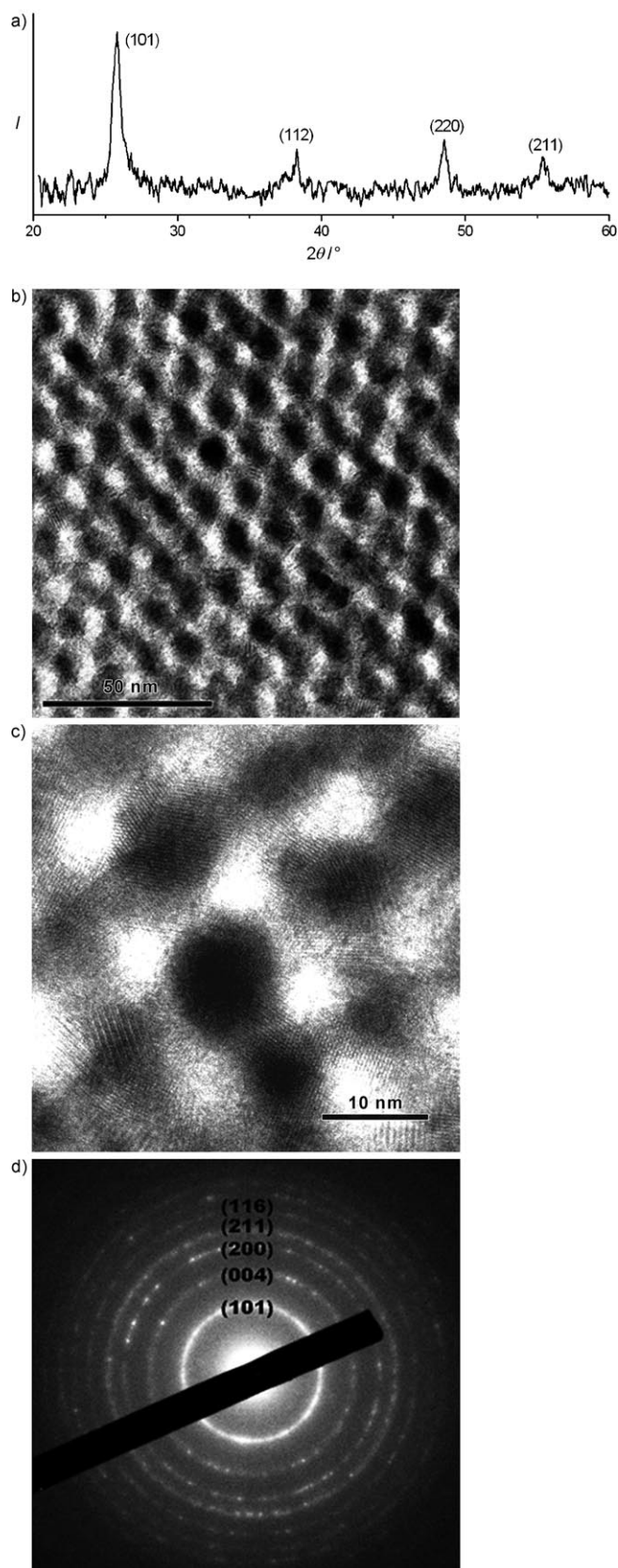
a)

b)

c)

d)

Figure 6. a) XRD pattern, b) low-magnification TEM image, c) high-magnification TEM image, and d) electron-diffraction pattern of a mesoporous titania thin film calcined at 500 °C.

low-angle XRD pattern does not show any peak, which indicates the absence of mesoscopic periodicity in the vertical direction. Therefore, the high-temperature calcination seems to cause the collapse of the mesostructure, but the collapse occurs only along the vertical direction so that the lateral ordering remains intact, which is possible because of the [111] orientation. In fact, this high-temperature calcination may be the way to produce truly 1D vertical channels, a possibility we are currently working on.

Conclusions

We have prepared mesoporous titania thin films that have many desirable features for future applications of nanodevices. It has large domains of highly ordered arrays of vertical channels. Most of the channels are accessible from the film surface. High-temperature treatment can convert the wall material from amorphous titania into anatase without losing the ordered mesoporous structure. Most of these features appear to originate from the [111] orientation of the $Im\bar{3}m$ structure in the as-cast film. With all these features combined, we believe that our mesoporous titania thin films can find application in the fabrication of nanodevices.

Experimental Section

The MTTFs were formed by spin-coating a precursor solution, followed by aging and calcination. The precursor solution was prepared by dissolving $TiCl_4$ and F-127 in ethanol with vigorous stirring under ambient conditions. The composition of the solution was $TiCl_4$/F-127/EtOH = 1:0.004:22. After being cast onto substrates at a spinning rate of 4000–6000 rpm under a controlled atmosphere of 70% relative humidity and 25°C, the spin-cast films were aged at 18°C for 72 h at a relative humidity of 80% to afford a self-assembled mesostructure. The films were calcined at 400°C for 2 h to give mesoporous titania thin films free of organics. Electrochemical experiments were carried out in a conventional three-electrode cell with an MTTF-modified electrode as the working electrode, a standard Ag/AgCl electrode as the reference electrode, and a platinum plate as the counter electrode. The procedure for making the MTTF working electrodes have been described in the main text. The electrodeposition was conducted in an aqueous solution of $HAuCl_4$ (0.02 M) under an applied potential of 0.02 V for 5 s. Characterization of the thin films by XRD was carried out with a Rigaku D/max-RC diffractometer. High-resolution TEM images (JEOL-3011, 300 kV) were obtained on samples prepared by scraping off the films. Surface images of the thin films were obtained by FESEM (JSM6700F).

Acknowledgements

[1] K. L. Frindell, M. H. Bartl, A. Poitsch, G. D. Stucky, *Angew. Chem.* **2002**, *114*, 1001; *Angew. Chem. Int. Ed.* **2002**, *41*, 959.

[2] E. L. Crepaldi, G. J. de A. A. Soler-Illia, D. Grosso, F. Cagnol, F. Ribot, C. Sanchez, *J. Am. Chem. Soc.* **2003**, *125*, 9770.

[3] Y. K. Hwang, K. C. Lee, Y.-U. Kwon, *Chem. Commun.* **2001**, 1738.

[4] S. Y. Choi, B. Lee, D. B. Carew, M. Mamak, F. C. Peiris, S. Speakman, N. Chopra, G. A. Ozin, *Adv. Funct. Mater.* **2006**, *16*, 1731.

[5] U.-H. Lee, H. Lee, S. Wen, S.-I. Mho, Y.-U. Kwon, *Microporous Mesoporous Mater.* **2006**, *88*, 48.

[6] E. Lancelle-Beltran, P. Prené, C. Boscher, P. Belleville, P. Buvat, S. Lambert, F. Guillet, C Boissière, D. Grosso, C. Sanchez, *Chem. Mater.* **2006**, *18*, 6152.

[7] M. D. Perez, E. Otal, S. A. Bilmes, G. J. A. A. Soler-Illia, E. L. Crepaldi, D. Grosso, C. Sanchez, *Langmuir* **2004**, *20*, 6879.

[8] S. Y. Choi, M. Mamak, N. Coombs, N. Chopra, G. A. Ozin, *Nano Lett.* **2004**, *4*, 1231.

[9] K. M. Coakley, M. D. Mcgehee, *Chem. Mater.* **2004**, *16*, 4533.

[10] Y. Yamauchi, M. Sawada, A. Sugiyama, T. Osaka, Y. Sakka, K. Kuroda, *J. Mater. Chem.* **2006**, *16*, 3693.

[11] V. R. Koganti, D. Dunphy, V. Gowrishankar, M. D. McGehee, X. F. Li, J. Wang, S. E. Rankin, *Nano Lett.* **2006**, *6*, 2567.

[12] C.-W. Wu, T. Ohsuna, M. Kuwabara, K. Kuroda, *J. Am. Chem. Soc.* **2006**, *128*, 4544.

[13] U.-H. Lee, M.-H. Kim, Y.-U. Kwon, *Bull. Korean Chem. Soc.* **2006**, *27*, 808.

[14] S. Y. Choi, B. Lee, D. B. Carew, M. Mamak, F. C. Peiris, S. Speakman, N. Chopra, G. A. Ozin, *Adv. Funct. Mater.* **2006**, *16*, 1731.

[15] D. Zhao, J. Feng, Q. Huo, N. Melosh, G. H. Fredrickson, B. F. Chmelka, G. D. Stucky, *Science* **1998**, *279*, 548.

[16] D. Zhao, Q. Hou, J. Feng, B. F. Chmelka, G. D. Stucky, *J. Am. Chem. Soc.* **1998**, *120*, 6024.

[17] Y. Lu, R. Ganguli, C. A. Drewien, M. T. Anderson, C. J. Brinker, W. Gong, Y. Guo, H. Soyez, B. Dunn, M. H. Huang, J. I. Zink, *Nature* **1997**, *389*, 364.

[18] D. Grosso, G. J. de A. A. Soler-Illia, E. L. Crepaldi, F. Cagnol, C. Sinturel, A. Bourgeois, A. Brunet-Bruneau, H. Amenitsch, P. A. Albouy, C. Sanchez, *Chem. Mater.* **2003**, *15*, 4562.

[19] J. Tang, Y. Y. Wu, E. W. McFarland, G. D. Stucky, *Chem. Commun.* **2004**, 1670.